https://doi.org/10.5194/bg-2020-89
Preprint. Discussion started: 21 April 2020

Biogeosciences Discussions
Open Access

Variations in diurnal and seasonal net ecosystem carbon dioxide exchange in a semiarid sandy grassland ecosystem in China's Horqin Sandy Land

Yayi Niu[a,b,c,e], Yuqiang Li[a,b,c,*], Hanbo Yun[a,d,e], Xuyang Wang[a,b,c], Xiangwen Gong[a,b], Yulong Duan[a,b,c], Jing Liu[a]

[a] Northwest Institute of Eco-Environment and Resources, Chinese Academy of Sciences, Lanzhou 730000, China

[b] University of Chinese Academy of Sciences, Beijing 100049, China

[c] Naiman Desertification Research Station, Northwest Institute of Eco-Environment and Resources, Chinese Academy of Sciences, Tongliao 028300, China

[d] State Key Laboratory of Frozen Soil Engineering, Northwest Institute of Eco-Environment and Resources, Chinese Academy of Sciences, Lanzhou, Gansu 730000, China

[e] Center for Permafrost (CENPERM), Department of Geosciences and Natural Resource Management, University of Copenhagen, DK-1350 Copenhagen, Denmark

* *Correspondence to*: Yuqiang Li (liyq@lzb.ac.cn)

Abstract

Grasslands are major terrestrial ecosystems in arid and semiarid regions, and play important roles in the regional carbon dioxide (CO_2) balance and cycles. Sandy grasslands are sensitive to climate change, yet the magnitudes, patterns, and environmental controls of their CO_2 flows are poorly understood. Here, we report the results from continuous year-round CO_2 observations in 5 years from a sandy grassland in China's Horqin Sandy Land. The sandy grassland was a net CO_2 source at an annual scale, with a mean annual net ecosystem CO_2 exchange (NEE) of 48.88 ± 8.10 g C m^{-2} yr^{-1} in the years for which a complete dataset was available (2015, 2016, and 2018); total annual precipitation was the most important factor for NEE. At a seasonal scale, the sandy grassland showed net CO_2 absorption during the summer, but net CO_2 release in the other seasons. The main environmental factors that affected NEE were temperature and soil water content (SWC) in the spring, soil heat flux and solar radiation in the summer, soil heat flux and temperature in autumn, and SWC and temperature in winter. At the diurnal scale, net solar radiation was the most important factor for NEE in all seasons. The sandy grassland may have been a net annual CO_2 source at an annual scale because the study site is recovering from degradation, thus vegetation productivity is still low. Therefore, the ecosystem has not yet transitioned to a CO_2 sink and long-term observations will be necessary to reveal the true source or sink intensity and its response to environmental and biological factors.

Keywords: Net ecosystem CO_2 exchange (NEE); Gross primary productivity (GPP); ecosystem respiration (R_{ec}); Eddy covariance; Horqin Sandy Land

1 Introduction

Arid and semiarid ecosystems cover 30 to 40 % of the global terrestrial surface (Poulter et al., 2014). The extent and distribution of these areas are increasing in response to factors such as climate change, changes in wildfire frequency and intensity, and changes in land use (Asner et al., 2003; Hastings et al, 2010). These ecosystems are important because they account for 30 to 35 % of terrestrial net primary productivity (Gao et al., 2012; Liu et al., 2016a) and approximately 15 % of the global soil organic carbon pool (Lal, 2004; Liu et al., 2016a). Thus, the high potential carbon sequestration in arid and semiarid areas may have a greater impact on the future global carbon cycle than sequestration in tropical rainforest areas (Emmerich, 2003; Nosetto et al., 2006; Poulter et al., 2014), and arid and semiarid ecosystems will have significant effects on the global carbon cycle and carbon balance (Lal, 2004). However, arid and semiarid ecosystems have received much less attention than wetter ecosystems, and the lack of high-frequency continuous observations has led to a weak understanding of their role in global terrestrial net ecosystem CO_2 exchange (NEE) (Baldocchi et al., 2001; Hastings et al., 2010).

Desertification occurs in more than two-thirds of the area of arid and semiarid ecosystems (Lal, 2001). This may cause a serious imbalance in the structure and function of these ecosystems (Huenneke et al., 2002; Vest et al., 2011), especially in terms of whether the ecosystem functions as a carbon source or sink (Shachak et al., 1998; Gang et al., 2011). Grazing exclusion is a common method used to combat desertification in the world's arid and semiarid areas (Mureithi et al., 2010; Sousa et al., 2012). For example, Sun et al. (2015) suggested that proper exclosures promoted the recovery of degraded sandy grassland and more sustainably use sandy grassland resources.

The Horqin Sandy Land is the largest sandy land in China, and nearly 80% of the area has been desertified (Li et al., 2019). The sandy land includes multiple overlapping ecotones, including transition zones between areas with different population pressures, between semi-humid and semiarid areas, and typical agro-pastoral ecotones. The ecological environment is fragile and extremely sensitive to climate change and human activities (Bagan et al., 2010; Zhao et al., 2015). The region's sandy grassland grows on aeolian sandy soils or with sandy soils as the substrate, and is typical of the grassland vegetation that develops in sandy land. This grassland ecosystem is widespread in the Horqin Sandy Land (Munkhdalai et al., 2007; Zhao et al., 2007). Research showed that the restoration of degraded sandy grassland can increase its productivity and carbon sequestration, and that the ecosystem can begin to act as a carbon sink (Ruiz-Jaen and

Aide, 2005; Zhao et al., 2016). However, other studies showed that it was a carbon source (Li et al., 2012; Niu et al., 2018). There have been relatively few long-term studies of sandy grassland at the ecosystem level, so we do not yet fully understand the characteristic of NEE and its components, gross primary productivity (GPP) and ecosystem respiration (R_{ec}), at an ecosystem scale, particularly for sandy grassland protected by grazing exclosures, and more data are needed, particularly for semiarid sandy land (Barrett, 1968; Czobel et al., 2012).

Precipitation is one of the factors that most strongly affects NEE in arid and semiarid areas. It affects NEE mainly through its effects on GPP and R_{ec} (Lal, 2004; Dasci et al, 2010; Hastings et al, 2010; Liu et al., 2016b). Previous research showed that reduced precipitation caused a continental-scale reduction in GPP, with concurrent decreases of R_{ec} (Ciais et al., 2005). In contrast, other studies found that GPP was more sensitive than respiration to precipitation (Thomas et al., 2010; Shi et al., 2014). For instance, Delgado-Balbuena et al. (2019) have shown that GPP was more than twice as sensitive as R_{ec} to precipitation in a semiarid grassland. The precipitation in the Horqin Sandy Land is low, with high temporal and spatial variation, and other water resources such as groundwater are small (Niu et al., 2015). Moreover, we found no reports on the response of ecosystem-scale NEE and its components to precipitation, and the response mechanisms are uncertain in the sandy grassland. Therefore, long-term data are required to fully understand how changes in annual precipitation influence the annual NEE, GPP, and R_{ec} of sandy grassland.

In this paper, we present the results from continuous (14 September 2014 to 31 December 2018) *in situ* monitoring of CO_2 dynamics in the Horqin Sandy Land's sandy grassland using the eddy covariance technique, and quantified the temporal variation of NEE and the factors that control it. We had the following goals: (1) To quantify the diurnal, seasonal, and annual variation in NEE, GPP, and R_{ec}. (2) To identify the environmental factors that controlled NEE and its components at different temporal scales, and the possible underlying mechanisms in the sandy grassland. (3) To determine how annual precipitation affects the annual ecosystem NEE, GPP, and R_{ec}.

https://doi.org/10.5194/bg-2020-89
Preprint. Discussion started: 21 April 2020

Biogeosciences Discussions

2 Materials and methods

2.1 Experimental site

Our study was conducted in a sandy grassland in the southern part of the Horqin Sandy Land, Inner Mongolia, China, at the Naiman Desertification Research Station of the Chinese Academy of Sciences (42°55′ N, 120°42′ E) (Fig. 1). The terrain is flat, and it evolved from reclamation of sandy grassland for agriculture to severe desertification, after which cultivation was abandoned and grazing exclosures were established to allow natural recovery of the vegetation, starting in 1985 (Zhao et al., 2007). Thus, the grassland had been recovering naturally for nearly 30 years when our study began. At an elevation of 377 m a.s.l., the study area has a continental semiarid monsoon temperate climate regime. The mean annual temperature is 6.8 ℃, with mean monthly temperatures ranging from -9.63 ℃ in January to 24.58 ℃ in July. Average annual precipitation is approximately 360 mm, with 70% of the precipitation occurring during the growing season, between June and August. Annual mean potential evaporation is approximately 1973 mm. The annual frost-free period is 130 to 150 days. The zonal soil is a sandy chestnut soil, but most of the soil has been degraded by a combination of climate change and anthropogenic activity (unsustainable grazing or agriculture) into an aeolian sandy soil under the action of wind erosion (Zhao et al., 2007), with coarse sand, fine sand, and clay-silt contents of 92.7, 3.3, and 4.0 % in the topsoil to a depth of 20 cm. The contents of soil organic carbon and total nitrogen were 1.27 and 0.21 g kg^{-1}, respectively. Vegetation cover in the study area ranged from 50 to 70 %. The dominant plant species were annual herbs, including *Artemisia scoparia, Setaria viridis, Salsola collina,* and *Corispermum hyssopifolium* (Niu et al., 2018).

2.2 Eddy covariance observations

An eddy covariance flux tower (2.0 m high) was installed at the center of the observation field (Fig. 1b, c). We have continuously monitored CO_2, water, and heat fluxes at the tower using the eddy covariance system since late 2014. The fetch from all directions was more than 200 m. Calculations with a footprint model indicated that the fetch was well within the desired flux footprint (Schmid, 1994; Xu and Baldocchi,

https://doi.org/10.5194/bg-2020-89
Preprint. Discussion started: 21 April 2020

2004). The eddy covariance system consisted of an LI-7500 infrared gas analyzer (Li-Cor Inc., Lincoln, NE, USA), with a precision of 0.01 μmol m^{-2} s^{-1} and an accuracy within 1 % of the reading for measurements at 30-min mean intervals, and a CSAT-3 three-dimensional ultrasonic anemometer (Campbell Scientific, Inc., Logan, UT, USA), with a precision of 0.1 ℃ and an accuracy of 1 % for the readings at 30-min mean intervals. Raw 10-Hz data were recorded by a CR3000 datalogger (Campbell Scientific). The operation, calibration, and maintenance of the eddy covariance system followed the manufacturers' standard procedures. The LI-7500 was calibrated every 6 months for CO_2, water vapor, and dew point values using calibration gases and dew point generator measurements supported by the China Land–Atmosphere Coordinated Observation System (Yun et al., 2018). We cleaned the mirror of the LI-7500 every 15 days to maintain the automatic gain control value below its threshold (55 to 65). All of the instruments were powered by solar panels connected to a battery.

2.3 Micrometeorological measurements

Along with the flux measurements obtained by the eddy covariance equipment, we measured standard meteorological and soil parameters continuously with an array of sensors. A propeller anemometer was installed at the top of the meteorological tower to measure the wind speed and direction. Net radiation (R_n, W m^{-2}) was measured by a four-component radiometer (CNR-1, Kipp and Zonen, Delft, the Netherlands) installed at 1 m above the ground. The air temperature (T_{air}, °C) and relative humidity (%) instruments (HMP45C, Vaisala Inc., Helsinki, Finland) were mounted at 2 m above the ground to measure the T_{air}, relative humidity, and atmospheric pressure (kPa). Precipitation (mm) measurements were obtained from a meteorological station 400 m from the study site.

We installed five CS109 temperature probes (Campbell Scientific) and five CS616 moisture probes (Campbell Scientific) in the soil at depths of 10, 20, 30, 40, and 50 cm to measure soil temperature (T_{soil}, °C) and soil water content (SWC, %). Two self-calibrating HFP01 soil heat flux (SHF, W m^{-2}) sensors (Hukseflux, Delft, the Netherlands) were buried 5 and 10 cm below the ground to obtain the SHF data. All of the environmental parameters were measured simultaneously with the eddy covariance measurements, and all data were recorded as 30-min mean values with a CR3000 datalogger.

2.4 Data quality and gap-filling method

We used the EddyPro 6.2.0 software (https://www.licor.com/env/products/eddy_covariance/software.html) to process the 10-Hz raw eddy covariance data. Processing included spike removal, lag correction, secondary coordinate rotation, Webb–Pearman–Leuning correction, and sonic virtual temperature conversion (Webb et al., 1980). We used the data processing method of Lee et al. (2004) to process the 30-min mean raw flux measurements to ensure their quality. Processed data were further corrected for weather effects and sensor uncertainty using the following procedure: (1) We removed data gathered during precipitation events, power failures, and sensor maintenance or malfunction. (2) We excluded unrealistic CO_2 flux data (values outside the range of –2.0 to 2.0 mg CO_2 m^{-2} s^{-1}). (3) We rejected the data during stable atmospheric conditions at nighttime (friction velocity (u^*) < 0.1 m s^{-1}). Based on the R_n, NEE was classified as the daytime NEE_{day} ($R_n \geq 1$ W m^{-2}) or the night-time NEE_{night} ($R_n < 1$ W m^{-2}). This screening resulted in the rejection of 20 to 30 % of the flux data, depending on the period.

We used several strategies to compensate for missing data. We used linear interpolation to fill gaps that were shorter than 2 h. For longer gaps, we handled the gap in the NEE_{day} using the mean diurnal variation with a 7-day window (Falge et al., 2001), and handled the gap in the NEE_{night} using a temperature-dependent exponential model (Lloyd and Taylor, 1994):

$$NEE_{night} = R_0 \exp(b\, T_{10}) \qquad \text{Eq (1)}$$

where R_0 is the base ecosystem respiration rate when the soil temperature is 0 °C, b an empirically determined coefficient, and T_{10} is the soil temperature at a depth of 10 cm. Daytime ecosystem respiration can be estimated by extrapolation from the parameterization derived from Eq. (1). We did not attempt to fill in gaps longer than 7 days, and treated those gaps as missing data. Gross primary productivity (GPP) was

https://doi.org/10.5194/bg-2020-89
Preprint. Discussion started: 21 April 2020

obtained as follows:

$$GPP = NEE - R_{ec} \quad \text{Eq (2)}$$

We evaluated the data quality based on the degree of energy closure (sensible heat + latent heat – net radiation – soil heat flux). The energy closure values for the sandy grassland from 2015 to 2018 were 86.5, 82.1, 57.7, and 85.2 %, respectively.

2.5 Statistical analyses

We performed correlation analysis (Pearson's r) and principal-components analysis (PCA) using version 22 of the SPSS software (IBM, Armonk, NY, USA). Unless otherwise noted, we defined statistical significance at $p < 0.05$. Pearson's r was applied to confirm the strength of the relationships between parameters. PCA was used to identify the main environmental factors that affected NEE and its components at different temporal scales. Before performing PCA, we tested for collinearity (using a variance inflation factor of $0 < VIF < 10$) using the Kaiser–Meyer–Olkin (KMO) test and Bartlett's sphericity test. Collinearity was used to repartition the T_{soil} and SWC data. We considered KMO values > 0.50 and $p < 0.05$ for Bartlett's sphericity test to indicate acceptable data (Hair et al., 2005). Our data were suitable for PCA, with the KMO value ranging from 0.52 to 0.78 and $p < 0.001$ for all Bartlett's sphericity test results.

3 Results

3.1 Meteorological conditions

We recorded T_{air} in the sandy grassland between September 2014 and December 2018 (Fig. S1). The mean annual T_{air} was 7.38 °C, with minimum and maximum T_{air} of −17.82 and 27.15 °C, respectively. Average R_n was 74.13 W m^{-2}, with average minimum and maximum values for the 5 years minimum and maximum R_n of −13.09 and 166.32 W m^{-2}, respectively (Fig. S2). The diurnal- scale SHF values at depths of 5 and 10 cm were 0.65 and −0.21 W m^{-2}, respectively (Fig. S3), with maximum values of 34.43 and 26.88 W m^{-2} (both on 28 April 2018), and the minimum values were –36.26 and –23.77 W m^{-2} (both on 4 October 2016).

The annual mean T_{soil} values at depths of 10, 20, 30, 40, and 50 cm were 9.49, 9.66, 9.85, 10.22, and 10.65 °C (Fig. S4a). The average minimum diurnal values for the 5

https://doi.org/10.5194/bg-2020-89
Preprint. Discussion started: 21 April 2020

years diurnal T_{soil} at all depths were −18.08, −16.33, −14.17, −12.56, and −11.26 °C, respectively, and the average maximum diurnal values for the 5 years diurnal T_{soil} were 33.45, 32.31, 31.30, 30.49, and 29.76 °C, respectively. The annual mean SWC values at depths of 10, 20, 30, 40, and 50 cm were 3.5, 3.6, 4.2, 4.8, and 5.7 %, respectively (Fig. S4b). The average minimum diurnal values for the 5 years minimum diurnal SWC at all depths were 1.5, 1.6, 1.6, 2.4, and 2.7 %, respectively, and the average maximum diurnal values for the 5 years diurnal SWC were 10.8, 7.9, 11.0, 12.1, and 13.6 %, respectively.

The site was windy, with an annual average wind speed of 3.19 m s^{-1} from 2015 to 2018, and the principal direction of the strongest winds was from the northeast sector (Fig. S5). In spring, the average wind speed was 2.25 m s^{-1}. In summer, the average wind speed was about 2.51 m s^{-1}, predominantly driven by the north wind.

The annual precipitation totaled 212.3 mm in 2015, 276.8 mm in 2016, 312.8 mm in 2017, and 350.8 mm in 2018 (Fig. S4b). The mean annual precipitation was 288.2 mm, which was less than the mean annual precipitation of 360.0 mm from 1960 to 2014. During the spring (March, April, and May), precipitation was relatively abundant, with mean precipitation of about 41.9 mm, which accounted for 12 to 20 % of the total annual precipitation. The majority of the precipitation (about 65 %) occurred in the summer (June, July, and August), with mean precipitation of about 197.1 mm. The autumn (September, October, and November) precipitation was similar to that in spring, with a mean precipitation of about 48.6 mm, which accounted for 14 to 23 % of the annual total. During the winter (December, January, and February), the mean precipitation of 0.6 mm accounted for only 1 to 6 % of the annual total.

3.2 Annual, seasonal, and diurnal variability of NEE, GPP and R_{ec}.

Figure 2 suggests that the sandy grassland was a net CO_2 source, with an annual mean NEE, GPP, and R_{ec} of 48.88 ± 8.10, 351.78 ± 20.97, and 302.87 ± 28.96 g C m^{-2} yr^{-1} in the years for which a complete dataset was available (2015, 2016, and 2018). (We omitted 2017 from this calculation because of large gaps in the data, described below.) NEE ranged from 34.99 C m^{-2} yr^{-1} in 2018 to 63.05 g C m^{-2} yr^{-1} in 2015, whereas GPP ranged from 255.99 g C m^{-2} yr^{-1} in 2015 to 355.77 g C m^{-2} yr^{-1} in 2018 and R_{ec} ranged from 319.04 g C m^{-2} yr^{-1} in 2015 to 390.85 g C m^{-2} yr^{-1} in 2018. The eddy covariance tower was set up in mid-August 2014, and the instrument was allowed to stabilize for 1 month before we began collecting data, from 15 September to 23 December 2014; during that period, we measured a cumulative carbon release of 46.67 g C m^{-2}, with cumulative GPP and R_{ec} of 24.80 and 71.47 g C m^{-2}, respectively. From 15 February to 26 April 2017 and from 14 October to 6 November 2017, approximately 3 months of data were missing due to instrument maintenance and calibration, and the cumulative NEE, GPP, and R_{ec} were 63.33, 273.67 and 337.00 g C m^{-2} for the remaining 9 months of the year. Note that the periods covered by the data are therefore not identical.

We also observed clear seasonal variations in the total seasonal NEE, GPP, and R_{ec} (Fig. 3) and their diurnal cycles (Fig. 4). In spring, the sandy grassland was an atmospheric CO_2 source in all years, with NEE, GPP, and R_{ec} averaging 0.15 $\pm$0.05, 0.63 $\pm$0.03, and 0.78 $\pm$0.03 g C m^{-2} d^{-1}, respectively (Fig. 3a). The diurnal NEE cycle was characterized by a single absorption peak from around 07:30 to around 16:30 (Fig. 4a). Note that although all times in China are reported as the Beijing time, the study site was not sufficiently far east of Beijing for this to affect the physiological meaning of these times. The rest of the day was characterized by weak carbon absorption. The average diurnal GPP was also characterized by a single peak from around 05:00 to around 19:30, and the diurnal R_{ec} was characterized by an approximately horizontal line at about 0.78 g C m^{-2} d^{-1}. The maximum and minimum average diurnal values for NEE were 0.78 (20:00) and −0.81 (12:00) g C m^{-2} d^{-1}, respectively, versus 1.57 (12:00) and 0.58 (4:30) g C m^{-2} d^{-1} for GPP and 1.01 (18:00) and 0.05 (17:30) g C m^{-2} d^{-1} for R_{ec}.

In summer, the sandy grassland was a CO_2 sink in all years, with NEE, GPP, and R_{ec} averaging −0.58 $\pm$0.05, 2.44 $\pm$0.05, and 1.86 $\pm$0.03 g C m^{-2} d^{-1}, respectively (Fig. 3b). The diurnal cycles of NEE and GPP were also characterized by a single peak, between 05:00 and 19:30 (Fig. 4b), and the ecosystem CO_2 uptake reached its peak from around 10:30 to 12:00. The diurnal R_{ec} pattern was similar to the spring, but at a higher level (about 1.86 g C m^{-2} d^{-1}). The maximum and minimum diurnal NEE averaged 2.67

https://doi.org/10.5194/bg-2020-89
Preprint. Discussion started: 21 April 2020

(21:30) and −4.60 (11:30) g C m^{-2} d^{-1}, respectively, versus 6.02 (11:30) and 0.09 (19:30) g C m^{-2} d^{-1} for GPP and 2.77 (21:30) and 1.19 (8:00) g C m^{-2} d^{-1} for R_{ec}.

In autumn, the sandy grassland was a net source of atmospheric CO_2 in all years, with NEE, GPP, and R_{ec} averaging 0.50 ± 0.02, 0.27 ± 0.02, and 0.76 ± 0.02 g C m^{-2} d^{-1}, respectively (Fig. 3c). The diurnal dynamics of NEE, GPP, and R_{ec} in autumn (Fig. 4c) were similar to those in spring (Fig. 4a), but the magnitudes of NEE and GPP in autumn were lower than in the spring. The diurnal R_{ec} was similar to the spring, at about 0.76 g C m^{-2} d^{-1}. The maximum and minimum average diurnal NEE were 0.88 (19:00) and 0.02 (11:30) g C m^{-2} d^{-1}, respectively, versus 0.89 (17:30) and 0.63 (4:00) g C m^{-2} d^{-1} for GPP and 0.74 (12:00) and 0.01 (5:00) g C m^{-2} d^{-1} for R_{ec}.

In winter, the grassland ecosystem functioned as a net CO_2 source in all years, with an average seasonal NEE of 0.58 ± 0.01 g C m^{-2} d^{-1} (Fig. 3d). It should also be noted that since the investigation started on 14 September 2014 and ended on 31 December 2018, the 2017 to 2018 winter was only about one-third of the usual length (i.e., it did not include data from January and February 2019). The diurnal dynamics of the winter NEE differed from the other seasons (Fig. 4d), with a minimum release value of 0.38 g C m^{-2} d^{-1}, and with two emission peaks: at 0.81 g C m^{-2} d^{-1} (08:00) and 0.89 g C m^{-2} d^{-1} (16:30).

3.3 Response of NEE, GPP and R_{ec} to changes in environmental factors

We analyzed the effects of environmental factors on NEE and its components at different temporal scales. The analysis methods for the diurnal scale (Pearson's *r* and PCA) were the same as the methods used at a seasonal scale, so to avoid repetition, we have only described the relationship between the seasonal-scale NEE and its components and the associated environmental factors. At the diurnal scale, R_n was the main factor that affected NEE, GPP and R_{ec} in all four seasons (data not shown). NEE was significantly negatively correlated with R_n, whereas GPP and R_{ec} were positively correlated with R_n, indicating that the ecosystem's carbon sequestration capacity increased with increasing R_n.

Seasonal-scale NEE, GPP, and R_{ec} were significantly correlated with many

https://doi.org/10.5194/bg-2020-89
Preprint. Discussion started: 21 April 2020

Biogeosciences Discussions

environmental factors (Table S1). We found extremely weak and non-significant relationships between NEE, GPP, and R_{ec} and two climate variables (relative humidity and atmospheric pressure), so we excluded those variables from our subsequent analysis. NEE was negatively correlated with most environmental factors in all seasons except the autumn, when most correlations were positive, and GPP and R_{ec} were positively correlated with most environmental factors (Table S1).

In spring, T_{soil} at all depths, and T_{air}, R_n, and SWC at all depths were negatively correlated with NEE (Table S1). In the PCA, principal component 1 (PC1) explained 57 % of the NEE variation (Table 1), and was dominated by temperature (T_{soil} at all depths and T_{air}). PC2 explained about 25 % of the NEE variation, and was dominated by SWC at depths of 0 to 10 cm. The first two PCs explained about 82 % of the NEE variation. GPP was positively correlated with most environmental factors. PC1 explained 39 % of the GPP variation, and temperature and SWC at depths of 10 to 50 cm were the dominant factors (Table 2). PC2 explained about 33 % of GPP variation, and was dominated by SHF at all depths. The first three PCs explained about 89 % of the GPP variation. R_{ec} was positively correlated with all environmental factors except for wind speed. PC1 explained 42 % of the R_{ec} variation (Table 3) and was dominated by SWC at depth of 20 to 50 cm, T_{soil} at all depths, T_{air}, and R_n. PC2 explained about 30% of the R_{ec} variation, and was dominated by SHF at all depths. The first three PCs explained about 89 % of the R_{ec} variation.

In summer, PC1 explained 42 % of the NEE variation, and was dominated by SHF at all depths and R_n (Table 1). PC2 explained 29% of the NEE variation, and was dominated by air and soil temperatures. The first three PCs explained about 88 % of the NEE variation. For GPP, PC1 explained 36 % of the variation and was dominated by SHF at all depths and R_n (Table 2). PC2 explained 25% of the variation, and was dominated by air and soil temperatures. The first three PCs explained about 86 % of the GPP variation. For R_{ec}, PC1 explained 31 % of the variation and was dominated by SWC at all depths and by precipitation (Table 3). PC2 also explained 31 % of the variation, but was dominated by air and soil temperatures. The first three PCs explained

https://doi.org/10.5194/bg-2020-89
Preprint. Discussion started: 21 April 2020

about 78 % of the R_{ec} variation.

In autumn, PC1 explained 46 % of the NEE variation and was dominated by T_{air}, SWC at depth of 10 cm, T_{soil} at all depths, and R_n (Table 1). PC2 explained 34 % of the variation and was dominated by SWC at depths of 0 to 30 cm. The first two PCs explained about 80 % of the NEE variation. For GPP, PC1 explained 33 % of the variation and was dominated by SHF at all depths and T_{air} (Table 2). PC2 explained 28 % of the variation and was dominated by SWC and T_{soil} at all depths and R_n. The first four PCs explained about 85 % of the GPP variation. For R_{ec}, PC1 explained 36 % of the variation and was dominated by SHF at all depths and T_{air} (Table 3). PC2 explained 32% of the variation and was dominated by SWC and T_{soil} at all depths and by R_n. The first three PCs explained about 82 % of the R_{ec} variation.

In winter, the NEE were equal to R_{ec}. PC1 for NEE (R_{ec}) explained 39 % of the variation and was dominated by SWC at depths of 20 to 30 cm and T_{soil} at all depths (Table 1 and Table 3). PC2 accounted for 25 % of the variation and was dominated by SHF at a depth of 10 cm and T_{air}. For GPP, there was no photosynthesis during the winter, so no data is provided in Table 2.

In summary, the dominant control factors for NEE, GPP, and R_{ec} differed among the seasons.

4 Discussion

4.1 Annual and seasonal mean and diurnal variability

Our results suggested that the sandy grassland ecosystem in China's Horqin Sandy Land was a net CO_2 source, with an annual mean NEE of 48.88 ± 8.10 g C m^{-2} yr^{-1} in the years for which a complete dataset was available (2015, 2016, and 2018). This result was similar to that obtained for a semi-desert sandy grassland near Vácrátót, Hungary (where the dominant species were *Festuca vaginata* and *Stipa capillata*), but the Hungarian annual NEE was higher, at 131.48 g C m^{-2} yr^{-1} in 2001 (Balogh et al., 2005). In contrast, many other arid and semiarid dry ecosystems with similar climate and geographical conditions were a significant net sink for CO_2. For example, in the Mojave Desert ecosystem in the United States, where the dominant species were evergreen

https://doi.org/10.5194/bg-2020-89
Preprint. Discussion started: 21 April 2020

shrubs, drought-deciduous shrub species, and perennial grasses, the annual NEE was −102 ± 67 and −110 ± 70 g C m^{-2} yr^{-1} in 2005 and 2006, respectively (Wohlfahrt et al., 2008). China's Tengger Desert, where the dominant vegetation was xerophytic shrubs planted in 1956, had annual NEE of −13.87 and −23.36 g C m^{-2} yr^{-1} in 2009 and 2010, respectively (Gao et al., 2012). The southern edge of China's Mu Us desert, which is dominated by a mixture of deciduous shrub species, had an annual NEE of −77 g C m^{-2} yr^{-1} in 2012 (Jia et al., 2014). China's Gurbantonggut Desert, which is dominated by shrubs and grasses, had an annual NEE of −5 and −40 g C m^{-2} yr^{-1} in 2006 and 2007, respectively (Liu et al., 2016a). The reason for these differences from the present study may be differences in the carbon sequestration ability of the dominant vegetation. Zheng et al. (2007) showed that the average carbon sequestration of terrestrial higher plants was higher for shrubs than for herbs. The dominant vegetation of our study area comprised annual herbs, which would have lower carbon sequestration capacity than in a shrub-dominated ecosystem.

The sandy grassland ecosystem in the present study was a net CO_2 source at an annual scale. On the one hand, this is because the dominant plants were annual plants, with a low carbon sequestration capacity. On the other hand, the site is still recovering from severe degradation, and has relatively low vegetation productivity (e.g., the mean annual GPP (351.78 ± 20.97 g C m^{-2} yr^{-1}) in our study was lower in China's Mu Us desert (456 ± 20.97 g C m^{-2} yr^{-1}) (Jia et al., 2014)), and the restoration of degraded sandy grassland ecosystems is a long process (Li et al., 2019). Therefore, the ecosystem has not yet reached the threshold at which it will change into a CO_2 sink, and it will be necessary to study NEE for a longer period to reveal when that change occurs and the ecosystem's long-term response to environmental and biological factors (Su et al., 2003; Niu et al., 2018).

We believe that seasonal variation of environmental factors also explained the seasonal differences in NEE, GPP, and R_{ec} at our site. In spring, the sandy grassland was a net CO_2 source in all years (Fig. 3a). Before the growing season, plants begin to germinate, and both GPP and R_{ec} increased with increasing temperature, solar radiation,

https://doi.org/10.5194/bg-2020-89
Preprint. Discussion started: 21 April 2020

and precipitation (Niu et al., 2011; Rey et al., 2011). However, R_{ec} was more responsive than GPP to precipitation. Liu et al. (2016a) showed that precipitation before the growing season had an important impact on NEE in arid and semiarid regions. After the winter drought, the spring precipitation greatly promoted the respiration of soil microbes (Zhang et al., 2016). As a result, R_{ec} increased significantly. Precipitation also promoted GPP to some extent, but the carbon uptake was relatively small during plant germination. Therefore, the ecosystem was a net CO_2 source.

In summer, the sandy grassland was a CO_2 sink in all years (Fig. 3b). Our results agree with previous results for the study area (Li et al., 2015), as well as with results for a semiarid savanna in Australia (Hutley et al., 2005) and a grassland in California (Ma et al., 2007). GPP and R_{ec} increased because of the favorable temperature and moisture conditions. However, because photosynthesis is greater than respiration during the peak of the growing season, the ecosystem became a net CO_2 sink (Kemp, 1983; Liu et al., 2016a; Niu et al., 2018).

In the autumn and winter, the sandy grassland was a net CO_2 source in all years (Fig. 3c,d). At the end of the growing season (in autumn), annual plants began to die and photosynthesis weakened (Fang et al., 2014). As a result, the ecosystem gradually transformed from a carbon sink to a carbon source (Keenan et al., 2009; Kiely et al., 2009).

At the diurnal scale, NEE in the spring, summer, and autumn showed CO_2 uptake during the day (06:00-18:00), and CO_2 emission during the night (Fig. 4a, b, c). The NEE increased with increasing light intensity during the day, reached its peak value around noon, then decreased until sunset, when the ecosystem changed from net carbon absorption to carbon release (Wagle and Kakani, 2014; Jia et al., 2014).

In winter, the sandy grassland ecosystem showed CO_2 emission throughout the day (Fig. 4d). At a diurnal scale, the ecosystem showed carbon "uptake", at a level too small to display in Fig. 4d. This phenomenon may have resulted from heating effects in the open-path infrared gas analyzer (Burba et al., 2008). We recently created a Li-Cor LI-8150 gas analyzer system with six long-term monitoring chambers in the footprint of eddy covariance to test whether that hypothesis is correct.

4.2 Impacts of the environment on NEE, GPP, and R_{ec}

Our results demonstrated the important roles of the environmental factors in regulating the direction and amount of NEE between the atmosphere and the ecosystem in a sandy grassland in the Horqin Sandy Land. The most important environmental factors differed among the different scales.

At the diurnal scale, NEE in the four seasons was mainly explained by the R_n, which agrees with results for a study of the Mojave Desert ecosystem (Wohlfahrt et al., 2008). Our study area was located at a relatively high latitude, which means that solar radiation may be a limiting factor on many ecosystem processes such as GPP (Li et al., 2005; Liang et al., 2012).

At the seasonal scale, the carbon cycle processes were affected by many environmental factors, including soil and air temperatures, SWC, solar radiation (R_n and SHF), and precipitation. Our results showed that the dominant environmental factors that affected NEE differed among the seasons. Our PCA analysis (Tables 1, 2 and 3) showed that in the spring, the main environmental factors that affected NEE, GPP, and R_{ec} were temperature and SWC. After experiencing the winter cold and drought, the effect of temperature and SWC on soil thawing and vegetation greenup were greater than those of other environmental factors (Chu et al., 2013; Wolf et al., 2016).

In summer, the most important environmental factors for NEE and GPP were solar radiation and SHF. This result agreed with previous studies, which demonstrated that solar radiation was the main environmental factor that affected photosynthesis during the peak of the growing season (Saigusa et al., 2008; Hinko-Najera et al., 2017). However, SWC was the most important factor for R_{ec}, and the variation of SWC was mainly controlled by precipitation (Fig. S4b). Studies have suggested that the burst-type precipitation could strongly stimulate R_{ec} during the growing season in semiarid areas (Hunt et al., 2002; Saetre and Stark, 2005).

In autumn, SHF and air and soil temperatures were the dominant environmental

https://doi.org/10.5194/bg-2020-89
Preprint. Discussion started: 21 April 2020

factors for NEE, GPP, and R_{ec}. The ecosystem was dominated by R_{ec} during the later stages of the growing season, and studies have shown that R_{ec} was strongly affected by soil temperature (Wang et al., 2012; Niu et al., 2018), and that the changes of soil temperature depended on SHF (Gao et al., 2010; Guo et al., 2011). Therefore, SHF and temperature were the most important environmental factors for the autumn NEE, GPP, and R_{ec}.

In winter, the annual plants had withered, so there was no GPP and the entire ecosystem was characterized by carbon emission. Our results showed that SWC and soil temperature were the most important factors that affected NEE, and that NEE increased with decreasing SWC and temperature. Previous studies found that when SWC decreases sufficiently to create water stress, it may replace temperature as the main factor that controls soil respiration in arid and semiarid areas, and as a result, soil respiration decreased with decreasing SWC (Wu et al., 2010; Escolar et al., 2015). Our results were inconsistent with these previous studies. This may be due to drought, since precipitation during the winter amounted to between 1 and 6 % of the annual precipitation, and this would be exacerbated by strong winter winds in the Horqin Sandy Land (Fig. S5; Wang et al., 2005; Liu et al., 2016b). The soil organic matter and nutrients would also be lost faster when SWC decreases and the wind strengthens, resulting in increased carbon emission (Lai, 2004; Munodawafa, 2011).

We also analyzed the relationship between annual NEE, GPP, and R_{ec} in the years for which a complete dataset was available (2015, 2016, and 2018) and the environmental factors (Table S1). We found that the total annual precipitation was the most important factor that limited NEE, GPP, and R_{ec}. NEE was negatively correlated with annual precipitation, GPP was positively correlated with it, and the correlation between R_{ec} and precipitation was not significant. Taken together, these results indicated different sensitivity of GPP and R_{ec} to annual precipitation.

Previous studies suggested that GPP was limited by the availability of water and was strongly correlated with total annual precipitation in arid and semiarid ecosystems (Webb et al., 1987; Sala et al., 1988). GPP of annual herbaceous plants was especially

https://doi.org/10.5194/bg-2020-89
Preprint. Discussion started: 21 April 2020

strongly affected by precipitation, which could change the composition and community structure of plants, thereby affecting GPP (Nackley et al., 2014; Wang et al., 2016). Our result was consistent with these previous studies. However, the correlation between R_{ec} and precipitation was not significant in our study. This may be because of the relatively high latitude of our study area, since R_{ec} was affected by multiple environmental factors that would be affected by latitude, such as temperature and solar radiation. However, we must improve our understanding of the responses of the ecosystem to precipitation and the underlying mechanisms that control whether it will be a carbon source or sink. To accomplish this, it will be necessary to observe the ecosystem continuously for a longer period of time.

5 Conclusions

Our field data indicated that the sandy grassland has functioned as a CO_2 source at an annual scale, with a mean annual NEE of 48.88 ± 8.10 g C m^{-2} yr^{-1}. At the seasonal scale, the sandy grassland showed net CO_2 absorption during the summer, but net CO_2 release in the other seasons. At the diurnal scale, the ecosystem showed a strong single daytime absorption peak in the spring, summer, and autumn, but strong CO_2 emission at night. In winter, the ecosystem was characterized by CO_2 emission all day, as there was no GPP.

At the daily scale, NEE in all four seasons was controlled by R_n. At the seasonal scale, NEE was mainly affected by temperature and SWC in the spring, solar radiation in the summer, SHF and temperature in the autumn, and SWC and temperature in the winter. At the annual scale, the total annual precipitation was the most important factor for NEE. Our findings demonstrated the importance of long-term, high-frequency field monitoring in sandy land to improve our understanding of CO_2 cycling and its likely responses to a changing climate. However, it will be necessary to study the NEE for a longer period to reveal its long-term response to environmental and biological factors.

Data availability. In agreement with the FAIR Data standards, the data used in this article are archived, published, and available in a dedicated repository: http://doi.org/10.4121/uuid:35deeb02-8165-49b7-af8d-160d537ae15a.

Competing interests. The authors declare that they have no conflict of interest.

Author contributions. YQL, YYN, HBY, XYW, and YLD designed the study; YYN, XWG, and JL performed the experiments. YYN and HBY analyzed the data. YYN drafted the manuscript. All co-authors had a chance to review the manuscript and contributed to discussion and interpretation of the data.

Acknowledgements. This research was supported by the National Key Research and Development Program of China (2017YFA0604803 and 2016YFC0500901), the National Natural Science Foundation of China (grants 31971466, 31560161, 31260089, and 31400392), the Chinese Academy of Sciences "Light of West China" Program (18JR3RA004), and the One Hundred Person Project of the Chinese Academy of Sciences (Y551821).

References

Asner, G. P., Archer, S., Hughes, R. F., Ansley, R. J., and Wessman, C. A.: Net changes in regional woody vegetation cover and carbon storage in Texas Drylands, 1937–1999, Global Change Biol., 9, 316–335, https://doi.org/10.1046/j.1365-2486.2003.00594.x, 2003.

Bagan, H., Takeuchi, W., Kinoshita, T., and Bao, Y. H.: Land cover classification and change analysis in the Horqin Sandy Land from 1975 to 2007, IEEE J. Sel. Topics in Applied Earth Observations and Remote Sensing, 3, 168-177. https://doi.org/10.1109/jstars.2010.2046627, 2010.

Baldocchi, D., Falage, E., Gu, L, H., Olson, R., Hollinger, D., Running, S., Anthoni, P., Bernhofer, C., Davis, K., Evans, R., Fuentes, J., Goldstein, A., Katul, G., Law, B., Lee, X. H., Malhi, Y., Meyers, T., Munger, W., Oechel, W., Paw, U. K. T., Pilegaard, K., Schmid, H. P., Valentini, R., Verma, S., Vesala, T., Wilson, K., and Wofsy, S.: Fluxnet: a new tool to study the temporal and spatial variability

https://doi.org/10.5194/bg-2020-89
Preprint. Discussion started: 21 April 2020

of ecosystem-scale carbon dioxide, water vapor, and energy flux densities, Bulletin of the American Meteorological Society., 82, 2415–2434. https://doi.org/10.1175/1520-0477(2001)082<2415:FANTTS>2.3.CO;2, 2001.

Balogh, J., Czóbel, S., Juhász, A., Fóti, S., Nagy, Z., and Tuba, Z.: Seasonal CO_2 exchange variations of temperate semi-desert grassland in Hungary, Photosynthetica, 43, 107-110, https://doi.org/10.1007/s11099-005-7110-0, 2005.

Barrett, G. W.: The effects of an acute insecticide stress on a semi-enclosed grassland ecosystem, Ecology, 49, 1019, https://doi.org/10.2307/1934487, 1968.

Burba, G. G., McDermitt, D. K., Grelle, A., and Daniel, J. A.: Addressing the influence of instrument surface heat exchange on the measurements of CO_2 flux from open-path gas analyzers, Global Change Biol., 14, 1854-1876, https://doi.org/10.1111/j.1365-2486.2008.01606.x, 2008.

Chu, J. M., Wang, Q., Fan, Z. P., and Li, F. Y.: Effects of soil moisture condition and freeze-thaw cycle on soil respiration of different land-use types in Horqin Sandy Land, Chinese Journal of Ecology (in Chinese), 32, 1399-1404, http://www.cje.net.cn/EN/, 2013.

Ciais, P. H., Reichstein, M., Viovy, N., Granier, A., Ogée, J., Allard, V., Aubinet, M., Buchmann, N., Bernhofer, C., Carrara, A., Chevallier, F., Noblet, N. D., Friend, A. D., Friedlingstein, P., Grünwald, T., Heinesch, B., Keronen, P., Knohl, A., Krinner, G., Loustau, D., Manca, G., Matteucci, G., Miglietta, F., Ourcival, J.

https://doi.org/10.5194/bg-2020-89
Preprint. Discussion started: 21 April 2020

M., Papale, D., Pilegaard, K., Rambal, S., Seufert, G., Soussana, J. F., Sanz, M. J., Schulze, E. D., Vesala, T., and Valentini, R.: Europe-wide reduction in primary productivity caused by the heat and drought in 2003, Nature, 437, 529-533, https://doi.org/10.1038/nature03972, 2005.

Czobel, S., Szirmai, O., Nemeth, Z., Gyuricza, C., Házi, J., Tóth, A., Schellenberger, J., Vasa, L., and Penksza, K.: Short-term effects of grazing exclusion on net ecosystem CO_2 exchange and net primary production in a Pannonian sandy grassland, Notulae Botanicae Horti Agrobotanici Cluj-Napoca, 40, 67-72, https://doi.org/10.15835/nbha4028300, 2012.

Dasci, M., Koc, A., Comakli, B., Kerim, G. M., Murat, C. M., and Ibrahim, E. H.: Importance of annual and seasonal precipitation variations for the sustainable use of rangelands in semi arid regions with high altitude, African Journal of Agricultural Research, 5, 2184-2191, https://doi.org/10.1016/S1671-2927(09)60212-1. 2010.

Delgado-Balbuena, J., Arredondo, J. T., Loescher, H. W., Pineda-Martínez, L. F., Carbajal, J. N., and Vargas, R.: Seasonal precipitation legacy effects determine the carbon balance of a semiarid grassland, JGR Biogeosciences, 124, 987-1000, https://doi.org/10.1029/2018JG004799, 2019.

Emmerich, W. E.: Carbon dioxide fluxes in a semiarid environment with high carbonate soils, Agric. For. Meteorol., 116, 91–102, https://doi.org/10.1016/s0168-1923(02)00231-9, 2003.

Escolar, C., Maestre, F. T , and Rey. A.: Biocrusts modulate warming and rainfall

https://doi.org/10.5194/bg-2020-89
Preprint. Discussion started: 21 April 2020

Biogeosciences Discussions
Open Access

exclusion effects on soil respiration in a semi-arid grassland, Soil Biol. Biochem., 80, 9-17, https://doi.org/10.1016/j.soilbio.2014.09.019, 2015.

Falge, E., Baldocchi, D., Olson, R., Anthoni, P., and Dolman, H.: Gap filling strategies for defensible annual sums of net ecosystem exchange, Agric. For. Meteorol. 107, 43-69, https://doi.org/10.1016/S0168-1923(00)00225-2, 2001.

Fang, S. X., Zhou, L. X., Tans, P. P., Ciais, P., Steinbacher, M., Xu, L., and Luan, T.: *In situ* measurement of atmospheric CO_2 at the four WMO/GAW stations in China, Atmos. Chem. Phys., 14, 27287-27326. https://doi.org/10.5194/acp-14-2541-2014, 2014.

Gang, C. C., Zhang, J., and Li, J. L.: The advances in the carbon source/sink researches of typical grassland ecosystem in China, Procedia Environ. Sci., 10, 1646-1653. https://doi.org/10.1016/j.proenv.2011.09.259, 2011.

Gao, Y. H., Li, X. R., Liu, L.C., Jia, R. L., Yang, H. T., Li, G., and Wei, Y. P.: Seasonal variation of carbon exchange from a revegetation area in a Chinese desert, Agric. For. Meteorol., 156, 134-142, https://doi.org/10.1016/j.agrformet.2012.01.007, 2012.

Gao, Z., Horton, R., and Liu, H. P.: Impact of wave phase difference between soil surface heat flux and soil surface temperature on soil surface energy balance closure, Journal of Geophysical Research Atmospheres, 115, 1-10 https://doi.org/10.1029/2009JD013278, 2010.

Guo, D. L., Yang, M. X., and Wang, H. J.: Sensible and latent heat flux response to diurnal variation in soil surface temperature and moisture under different

https://doi.org/10.5194/bg-2020-89
Preprint. Discussion started: 21 April 2020

freeze/thaw soil conditions in the seasonal frozen soil region of the central Tibetan Plateau, Environ. Earth Sci., 63, 97-107. https://doi.org/10.1007/s12665-010-0672-6, 2011.

Hair, J. F., Black, B., Babin, B., Anderson, R. E., and Tatham, R. L.: Multivariate data analysis, 6th Ed. New Jersey: Prentice Hall, 2005.

Hastings, S. J., Oechel, W. C., and Muhliamelo, A.: Diurnal, seasonal and annual variation in the net ecosystem CO_2 exchange of a desert shrub community (sarcocaulescent) in Baja California, Mexico. Global Change Biol., 11, 927-939, https://doi.org/10.1111/j.1365-2486.2005.00951.x. 2010.

Hinko-Najera, N., Livesley, S.J., Beringer, J., Isaac, P., van Gorsel, E., Exbrayat, J.F., McHugh, I., and Arndt, S.K.: Net ecosystem carbon exchange of a dry temperate eucalypt forest, Biogeosciences Discussions, 2016, 1-33. https://doi.org/10.5194/bg-2016-192. 2017.

Huenneke, L. F., Anderson, J. P., Remmenga, M., and Schlesinger, W. H.: Desertification alters patterns of aboveground net primary production in Chihuahuan ecosystems, Global Change Biol., 8, 247-264．https://doi.org/10.1046/j.1365-2486.2002.00473.x, 2002.

Hunt, J. E., Kelliher, F. M., McSeveny, T. M., and Byers, J. N.: Evaporation and carbon dioxide exchange between the atmosphere and a tussock grassland during a summer drought, Agric. For. Meteorol., 111, 65-82. https://doi.org/10.1016/S0168-1923(02)00006-0, 2002.

Hutley, L. B., Leuning, R., Beringer, J., and Cleugh, H. A.: The utility of the eddy

https://doi.org/10.5194/bg-2020-89
Preprint. Discussion started: 21 April 2020

covariance techniques as a tool in carbon accounting: tropical savanna as a case study, Austral. J. Bot., 53, 663. https://doi.org/10.1071/Bt04147, 2005.

Jia, X., Zha, T. S., Wu, B., Zhang, Y. Q., Gong, J. N., Qin, S. G., Chen, G. P., Kellomäki, S., and Peltola, H.: Biophysical controls on net ecosystem CO_2 exchange over a semiarid shrubland in northwest China, Biogeosciences, 11, 4679-4693. https://doi.org/ 10.5194/bg-11-4679-2014, 2014.

Keenan, T., García, R., Friend, A. D., Zaehle, S., Sabate, S.: Improved understanding of drought controls on seasonal variation in Mediterranean forest canopy CO_2 and water fluxes through combined *in situ* measurements and ecosystem modelling, Biogeosci. Discuss., 6, 2285-2329, https: https://doi.org/10.5194/bgd-6-2285-2009, 2009.

Kemp, P. R.: Phenological patterns of Chihuahuan desert plants in relation to the timing of water availability, Journal of Ecology, 71, 427-436. https://doi.org/10.2307/2259725, 1983.

Kiely, G., Leahy, P., Sottocornola, M., Laine, A., Mishurov, M., Albertson, J., and Carton, O.: Celticflux: measurement and modelling of greenhouse gas fluxes from grasslands and a peatland in Ireland. Irish Environmental Protection Agency, STRIVE Report 24, http://www.epa.ie/pubs/reports/research/climate/strivereport24.html, 2009.

Lal, R.: Potential of desertification control to sequester carbon and mitigate the greenhouse effect, Clim. Change, 51, 35–72. https://doi.org/110.1023/a:1017529816140, 2001.

https://doi.org/10.5194/bg-2020-89
Preprint. Discussion started: 21 April 2020

Lal, R.: Carbon sequestration in dryland ecosystems, Environ. Manage., 33, 528–544. https://doi.org/10.1007/s00267-003-9110-9, 2004.

Lee, X. H., Massman, W. J., and Law, B. E.: Handbook of micrometeorology, Springer, Berlin. Vol. 29 of the Atmospheric and Oceanographic Sciences Library, https://doi.org/10.1007/1-4020-2265-4, 2004.

Li, F. R., Wang, T., Zhang, A. S., and Zhao, L. Y.: Wind-dispersed seed deposition patterns and seedling recruitment of *Artemisia halodendron* in a moving sandy land, Annals of Botany, 96, 69-80, https://doi.org/10.1093/aob/mci150, 2005.

Li, F. R., Zhao, L. Y., Zhang, H., Zhang, T. H., and Shirato, Y.: Wind erosion and airborne dust deposition in farmland during spring in the Horqin Sandy Land of eastern Inner Mongolia, China. Soil Till. Res., 75, 121-130. https://doi.org/10.1016/j.still.2003.08.001, 2004.

Li, Y. Q., Wang X. Y., Chen, Y. P., Luo, Y. Q., Lian, J., Niu, Y. Y., Gong, X. W., Yang, H., and Yu, P. D.: Changes in surface soil organic carbon in semiarid degraded Horqin Grassland of northeastern China between the 1980s and the 2010s, Catena, 174, 217–226, https://doi.org/10.1016/j.catena.2018.11.021, 2019.

Li, Y, Q., Zhao, X, Y., Chen, Y, P., Luo, Y, Q., and Wang, S, K.: Effects of grazing exclusion on carbon sequestration and the associated vegetation and soil characteristics at a semi-arid desertified sandy site in Inner Mongolia, northern China, Can. J. Soil Sci., 92, 807-819, https://doi.org/10.4141/cjss2012-030, 2012.

Li, Y. Q., Zhao, X. Y., Wang, S. K., Zhang, F. X., Lian, J., Huang, W. D., and Qu, H.:

https://doi.org/10.5194/bg-2020-89
Preprint. Discussion started: 21 April 2020

Carbon accumulation in the bulk soil and different soil fractions during the rehabilitation of desertified grassland in Horqin Sandy Land (northern China), Pol. J. Ecol., 63, 88-101, https://doi.org/10.3161/15052249PJE2015.63.1.008, 2015.

Liang, H., Zhang, R. H., Liu, J. M., Sun, Z, A., and Cheng, X. H.: Estimation of hourly solar radiation at the surface under cloudless conditions on the Tibetan Plateau using a simple radiation model, Advances in Atmospheric Sciences, 29, 675-689, https://doi.org/ 10.1007/s00376-012-1157-1, 2012.

Liu, R., Cieraad, E., Li, Y., and Ma, J. J. E.: Precipitation pattern determines the inter-annual variation of herbaceous layer and carbon fluxes in a phreatophyte-dominated desert ecosystem, Ecosystems, 19, 601-614, https://doi.org/10.1007/s10021-015-9954-x, 2016a.

Liu, S. L., Kang, W. P., and Wang, T.: Drought variability in Inner Mongolia of northern China during 1960–2013 based on standardized precipitation evapotranspiration index, Environ. Earth Sci., 75, 145. https://doi.org/10.1007/s12665-015-4996-0, 2016b.

Lloyd, J., and Taylor, J. A.: On the temperature dependence of soil respiration, Functional Ecology, 8, 315-323, https://doi.org/10.2307/2389824, 1994.

Ma, S. Y., Baldocchi, D. D., Xu, L. K., and Hehn, T.: Inter-annual variability in carbon dioxide exchange of an oak/grass savanna and open grassland in California. Agric. For. Meteorol., 147, 157-171, https://doi.org/10.1016/j.agrformet.2007.07.008, 2007.

https://doi.org/10.5194/bg-2020-89
Preprint. Discussion started: 21 April 2020

Munkhdalai, Z. A., Feng, Z. W., Wang, X. K., and Sun, H. W.: Sandy grassland blowouts in Hulunbuir, northeast China: geomorphology, distribution, and causes, Progress in Natural Science: Materials International, 17, 68-73. https://doi.org/10.1080/10020070612331343227, 2007.

Munodawafa, A.: Maize grain yield as affected by the severity of soil erosion under semi-arid conditions and granitic sandy soils of Zimbabwe, Physics and Chemistry of the Earth Parts A/B/C, 36, 963-967, https://doi.org/10.1016/j.pce.2011.07.068, 2011.

Mureithi, S. M., Verdoodt, A., and Ranst, E. V.: Effects and implications of enclosures for rehabilitating degraded semi-arid rangelands: critical lessons from Lake Baringo Basin, Kenya, Land Degradation and Desertification: Assessment, Mitigation and Remediation, https://doi.org/10.1007/978-90-481-8657-0_9, 2010.

Nackley, L. L., Vogt, K. A., and Kim, S. H.: *Arundo donax* water use and photosynthetic responses to drought and elevated CO_2, Agric. Water Manage., 136, 13-22, https://doi.org/ 10.1016/j.agwat.2014.01.004, 2014.

Niu, C. Y., Musa, A., and Liu, Y.: Analysis of soil moisture condition under different land uses in the arid region of Horqin sandy land, northern China, Solid Earth, 6, 1157-1167, https://doi.org/10.5194/se-6-1157-2015, 2015.

Niu, S, L., Luo, Y, Q., Fei, S, F., and Montagnani, L.: Seasonal hysteresis of net ecosystem exchange in response to temperature change: patterns and causes, Global Change Biol., 17, 3102-3114, https://doi.org/10.1111/j.1365-

https://doi.org/10.5194/bg-2020-89
Preprint. Discussion started: 21 April 2020

2486.2011.02459.x, 2011.

Niu, Y. Y., Li, Y. Q., Wang, X. Y., Gong, X. W., Luo, Y. Q., and Tian, D.Y.: Characteristics of annual variation in net carbon dioxide flux in a sandy grassland ecosystem during dry years. Acta Prataculturae Sinica (in Chinese), 27, 215-221, https://doi.org/10.11686/cyxb2017231, 2018.

Nosetto, M. D., Jobbágy, E.G., and Paruelo, J. M.: Carbon sequestration in semi-arid rangelands: comparison of *Pinus ponderosa* plantations and grazing exclusion in NW Patagonia, J. Arid Environ., 67, 142-156, https://doi.org/10.1016/j.jaridenv.2005.12.008, 2006.

Poulter, B., Frank, D., Ciais, P., Myneni, R. B., Andela, N., Bi, J., Broquet, G., Canadell, J. G., Chevallier, F., and Liu, Y. Y.: Contribution of semi-arid ecosystems to interannual variability of the global carbon cycle, Nature, 509, 600–603, https://doi.org/10.1038/nature13376, 2014.

Rey, A., Pegoraro, E., Oyonarte, C., Were, A., Escribano, P., and Raimundo, J.: Impact of land degradation on soil respiration in a steppe (*Stipa tenacissima* L.) semi-arid ecosystem in the SE of Spain, Soil Biol. Biochem., 43, 393-403. https://doi.org/10.1016/j.soilbio.2010.11.007, 2011.

Ruiz-Jaen, M, C., and Aide, T. M.: Restoration success: how is it being measured? Restor. Ecol., 13, 569-577, https://doi.org/10.1111/j.1526-100X.2005.00072.x, 2005.

Saetre, P., and Stark, J. M.: Microbial dynamic sand carbon and nitrogen cycling following rewetting of soils beneath two semi-arid plant species, Oecologia,

https://doi.org/10.5194/bg-2020-89
Preprint. Discussion started: 21 April 2020

142, 247-260, https://doi.org/10.2307/20062160, 2005.

Saigusa, N., Yamamoto, S., Hirata, R., Ohtani, Y., Ide, R., Asanuma, J., Gamoa, M., Hirano,T., Kondo, H., Kosugi, Y., Li, S. G., Nakai, Y., Takagi, K., Tani, M., and Wang, H. M.: Temporal and spatial variations in the seasonal patterns of CO_2 flux in boreal, temperate, and tropical forests in East Asia, Agric. For. Meteorol., 148, 700-713, https://doi.org/10.1016/j.agrformet.2007.12.006, 2008.

Sala, O. E., Parton, W. J., Joyce, L. A., and Lauenroth, W.K.: Primary production of the central grassland region of the United States, Ecology, 69, 40–45. https://doi.org/10.2307/1943158, 1988.

Schmid, H. P.: Source areas for scalars and scalar fluxes. Boundary Layer Meteorol., 67, 293-318, https://doi.org/10.1007/BF00713146, 1994.

Shachak, M., Sachs, M., and Moshe, I.: Ecosystem management of desertified shrublands in Israel, Ecosystems, 1, 475-483. https://doi.org/10.1007/s100219900043, 1998.

Shi, Z., Thomey, M. L., Mowll, W., and Litvak, M.: Differential effects of extreme drought on production and respiration: synthesis and modeling analysis, Biogeosciences, 11, 621-633. https://doi.org/10.5194/bg-11-621-2014, 2014.

Sousa, F. P., Ferreira, T. O., Mendonça, E. S., Romero, R. E., and Oliveira, J. G. B.: Carbon and nitrogen in degraded Brazilian semi-arid soils undergoing desertification, Agric. Ecosyst. Environ., 148, 11-21. https://doi.org/10.1016/j.agee.2011.11.009, 2012.

Su, Y. Z., Zhao, H. L., and Zhang, T. H.: Influence of grazing and enclosure on carbon sequestration in degraded sandy grassland, Inner Mongolia (In Chinese), North China. Chinese Journal of Environmental Science, 46, 321-328. https://doi.org/10.1080/00288233.2003.9513560, 2003.

Sun, D. C., Li, Y. L., Zhao, X. Y., Zuo, X. A., and Mao, W.: Effects of enclosure and grazing on carbon and water fluxes of sandy grassland (in Chinese), Chinese Journal of Plant Ecology, 39, 565-576. https://doi.org/10.17521/cjpe.2015.0054, 2015.

Thomas, M. V., Malhi, Y., Fenn, K. M., and Fisher, J. B.: Carbon dioxide fluxes over an ancient broadleaved deciduous woodland in southern England, Biogeosciences, 8, 1595-1613, https://doi.org/10.5194/bg-8-1595-2011, 2010.

Vest, K. R., Elmore, A. J, Kaste, J. M., and Okin, G. S.: Functional connectivity as a possible indicator of desertification in degraded grasslands, Am. Geophys. Union Fall. Meeting. Abstract B51A-0383, 2011.

Wagle, P., and Kakani, V. G.: Environmental control of daytime net ecosystem exchange of carbon dioxide in switchgrass, Agric. Ecosyst. Environ., 186, 170-177, https://doi.org/10.1016/j.agee.2014.01.028, 2014.

Wang, X. M., Dong, Z. B., Yan, P., Zhang, J. Z., and Qian, G. Q.: Wind energy environments and dunefield activity in the Chinese deserts, Geomorphology, 65, 33-48, https://doi.org/10.1016/j.geomorph.2004.06.009, 2005.

Wang, X. Y., Li, Y. L., Zhao, X. Y., Mao, W., Cui, D., Qu, H., Lian, J., and Luo, Y. Q.: Responses of soil respiration to different environment factors in semi-arid and

https://doi.org/10.5194/bg-2020-89
Preprint. Discussion started: 21 April 2020

arid areas. Acta Ecologica Sinica (In Chinese), 32, 4890-4901. https://doi.org/10.5846/stxb201107281108, 2012.

Wang, Y. C., Alberto, B. C., Jiang, D. M., and Ala, M.: The role of sexual vs. asexual recruitment of *Artemisia wudanica* in transition zone habitats between inter-dune lowlands and active dunes in Inner Mongolia, China. Solid Earth, 7: 621-629. https://doi.org/10.5194/se-7-621-2016, 2016.

Webb, E. K., Pearman, G. I., and Leuning, R.: Correction of flux measurements for density effects due to heat and water vapor transfer, Q. J. Roy. Meteorol. Soc., 106, 85-100, https://doi.org /10.1002/qj.49710644707, 1980,

Webb, W., Szarek, S., Lauenroth, W., Kinerson, R., and Smith, M.: Primary productivity and water use in native forest, grassland, and desert ecosystem, Ecology, 59, 1239–1247, https://doi.org/10.2307/1938237, 1978.

Wohlfahrt, G., Fenstermaker, L. F., and Arnone, J.A. III: Large annual net ecosystem CO_2 uptake of a Mojave Desert ecosystem, Global Change Biol., 14, 1475-1487. https://doi.org/10.1111/j.1365-2486.2008.01593.x, 2008.

Wolf, S., Keenan, T. F., Fisher, J. B., Baldocchi, D. D., Desai, A. R., Richardson, A.D., Scott, R. L., Law, B. E., Litvak, M. E., Brunsell, N. A., Peters, W., and Laan-Luijkx, I. T.: Warm spring reduced carbon cycle impact of the 2012 US summer drought. PNAS, 113, 5880-5885. https://doi.org/10.1073/pnas.1519620113, 2016.

Wu, X., Yao, Z. N., Brüggemann, N., and Shen, Z. Y.: Effects of soil moisture and temperature on CO_2 and CH_4 soil atmosphere exchange of various land use/cover types in a semi-arid grassland in Inner Mongolia, China. Soil Biol. Biochem., 42, 773-787, https://doi.org/10.1016/j.soilbio.2010.01.013, 2010.

Xu, L. K., and Baldocchi, D. D.: Seasonal variation in carbon dioxide exchange over a Mediterranean annual grassland in California, Agric. For. Meteorol., 123, 79-96, https://doi.org/10.1016/j.agrformet.2003.10.004, 2004.

Yun, H. B., Wu, Q. B., Zhuang, Q. L., Chen, A. P., Yu, T., Lyu, Z., Yang, Y. Z., Jin, H. J., Liu, G. J., Qu, Y., and Liu, L. C.: Consumption of atmospheric methane by the Qinghai–Tibet Plateau alpine steppe ecosystem, Cryosphere, 9, 2803-2819. https://doi.org/10.5194/tc-12-2803-2018, 2018.

Zhang, B. W., Li, S., Chen, S. P., Ren, T. T., Yang, Z. Q., Zhao, H. L., Liang, Y., and Han, X. G.: Arbuscular mycorrhizal fungi regulate soil respiration and its response to precipitation change in a semiarid steppe, Sci. Rep., 6, 19990, https://doi.org/10.1038/srep19990, 2016.

Zhao, H. L., Li, Y. Q., and Zhou, R. L.: Effects of desertification on C and N storages in grassland ecosystem on Horqin sandy land (in Chinese), Chinese Journal of Applied Ecology, 18, 2412. https://doi.org/10.1360/yc-007-1324, 2007.

Zhao, X. Y., Wang, S. K., Luo, Y. Y., Huang, W. D., Qu, H., and Lian, J.: Toward sustainable desertification reversion: a case study in Horqin Sandy Land of northern China. Sciences in Cold and Arid Regions, 1, 23-28. https://doi.org/10.3724/SP.J.1226.2015.00023, 2015.

Zhao, Y. L., Song, Z. L., Xu, X. T., Li, Z. M., Guo, F. S., and Pan, W. J.: Nitrogen application increases phytolith carbon sequestration in degraded grasslands of North China, Ecol. Res., 31, 117-123, https://doi.org/10.1007/s11284-015-1320-0, 2016.

Zheng, W. J., Bao, W. K., Gu, B., He, X., and Leng, L.: Carbon concentration and its characteristics in terrestrial higher plants. Chinese Journal of Ecology (in Chinese), 26, 307-313, https://doi.org/10.3969/j.issn.1674-7895.2014.03.01, 2007.

https://doi.org/10.5194/bg-2020-89
Preprint. Discussion started: 21 April 2020

Figure captions

Fig. 1. Locations of the Horqin Sandy Land and the Naiman station. (b) and (c) are the covariance site at the Naiman station during the growing and dormant seasons, respectively.

Fig. 2. Annual patterns of daily net ecosystem CO_2 exchange (NEE), gross primary productivity (GPP), and ecosystem respiration (R_{ec}) from 2014 to 2018. Positive NEE values indicate net CO_2 release, whereas negative values indicate net CO_2 uptake by the ecosystem. Note that the initial measurements were from 15 September to 23 December 2014, so no data are available for the first part of 2014.

Fig. 3. Seasonal mean net ecosystem CO_2 exchange (NEE), gross primary productivity (GPP), and ecosystem respiration (R_{ec}) from 2014 to 2018: (a) spring (March, April, and May), (b) summer (June, July, and August), (c) autumn (September, October, and November), and (d) winter (December, January, and February). Note that the initial measurements were from 15 September to 23 December 2014, so no data are available for the first part of 2014.

Fig. 4. Diurnal changes in mean net ecosystem CO_2 exchange (NEE), gross primary productivity (GPP), and ecosystem respiration (R_{ec}) from 2014 to 2018: (a) spring (March, April, and May), (b) summer (June, July, and August), (c) autumn (September, October, and November), and (d) winter (December, January, and February). Note that the initial measurements were from 15 September to 23 December 2014, so the spring and summer data do not include the period before 15 September. The final measurements were obtained on 31 December 2018, so the winter period from 2017 to 2018 was only about one-third of the usual length (i.e., it did not include data from January and February 2019).

https://doi.org/10.5194/bg-2020-89
Preprint. Discussion started: 21 April 2020

Fig.1.

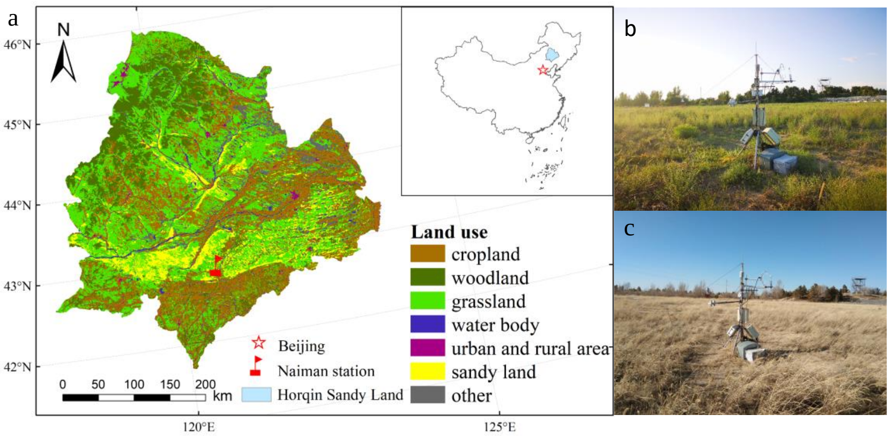

Fig. 2.

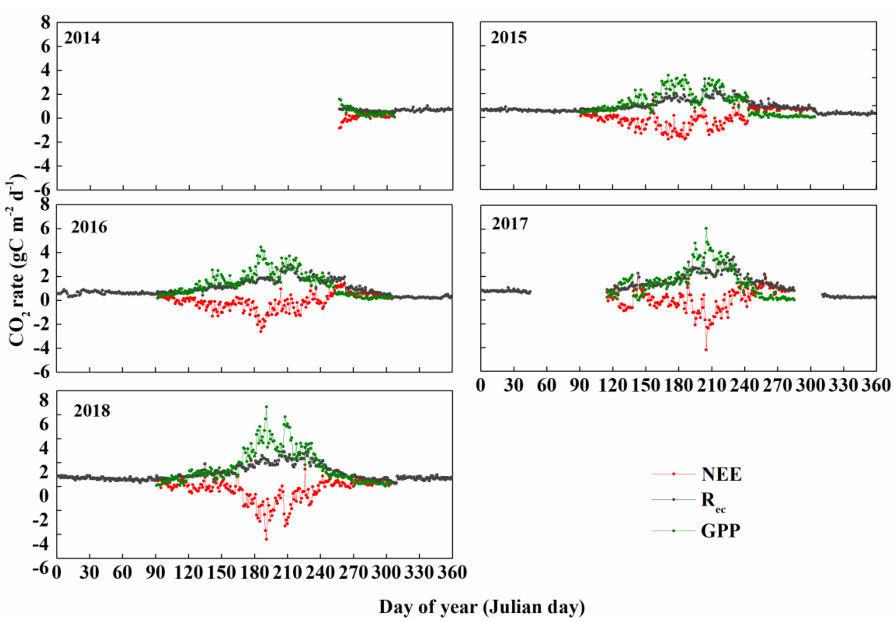

https://doi.org/10.5194/bg-2020-89
Preprint. Discussion started: 21 April 2020

Fig. 3.

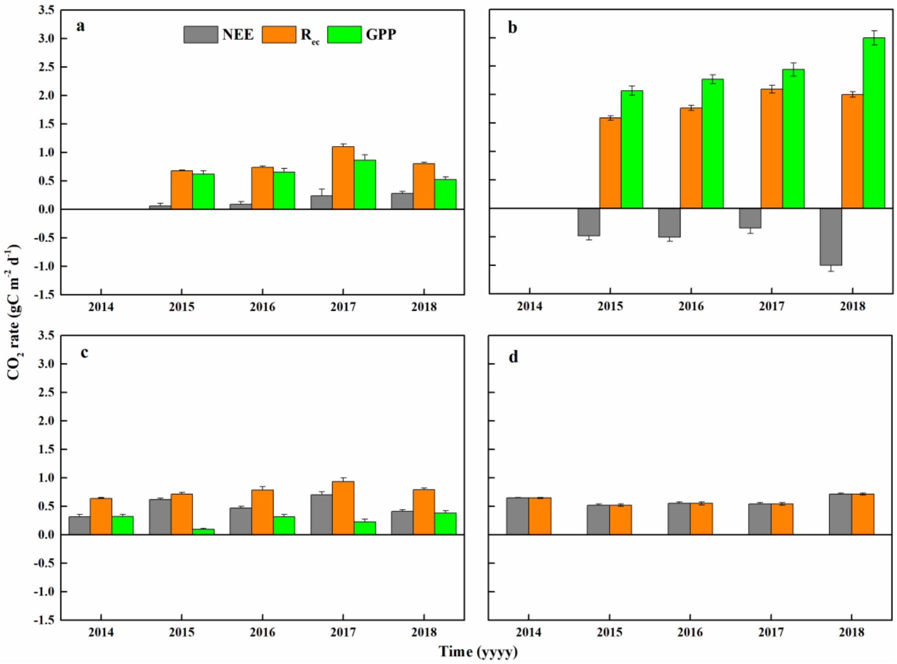

https://doi.org/10.5194/bg-2020-89
Preprint. Discussion started: 21 April 2020

Biogeosciences Discussions
Open Access

Fig. 4.

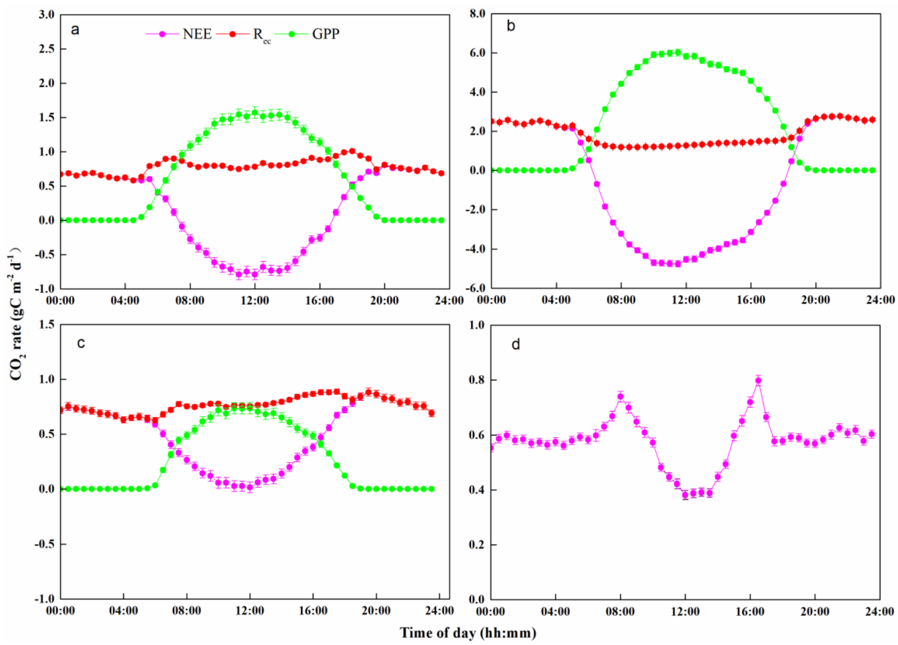

https://doi.org/10.5194/bg-2020-89
Preprint. Discussion started: 21 April 2020

Biogeosciences
Discussions
Open Access
EGU

Table 1. Principal-components analysis (PCA) for the relationships between the net ecosystem CO_2 exchange (NEE) and the environmental factors at a seasonal scale. PC, principal component; T_{air}, air temperature; R_n, net solar radiation; SHF, soil heat flux; SWC, soil water content; T_{soil}, soil temperature.

Component[a]	Spring		Summer			Autumn		Winter		
	PC1	PC2	PC1	PC2	PC3	PC1	PC2	PC1	PC2	PC3
T_{air}	0.910	0.188	0.423	0.861	-0.017	0.873	0.424	0.333	0.891	0.071
Wind speed								0.057	0.230	0.730
R_n	0.739	0.034	0.781	0.018	0.032	0.757	0.418	-0.106	0.320	-0.784
SHF at 5 cm			0.920	0.198	-0.036					
SHF at 10 cm			0.929	0.202	0.047	0.870	-0.072	-0.206	0.928	-0.090
SWC at 0-10 cm	0.112	0.978				0.238	0.824			
SWC at 10-30 cm						0.133	0.845			
SWC at 10-50 cm	0.780	0.510								
SWC at 20-30 cm								0.868	0.053	-0.144
SWC at 30-40 cm								0.949	-0.011	0.161
SWC at 40-50 cm			0.025	-0.052	0.998			0.880	-0.110	0.144
T_{soil} at 0-50 cm	0.935	0.140	-0.009	0.961	-0.055	0.780	0.508	0.735	0.390	0.244
Percent of variance	57.227	25.339	41.639	29.146	16.735	46.258	33.520	39.212	24.720	16.088
Cumulative	57.227	82.566	41.639	70.785	87.521	46.258	79.778	39.212	63.933	80.021

[a] Before the PCA, SWC was divided into six depth ranges (0 to 10, 10 to 30, 10 to 50, 20 to 30, 30 to 40, and 40 to 50 cm) according to the results of a collinearity test for the four seasons. T_{soil} was divided into a single range (0 to 50 cm) according to the results of a collinearity test for the different seasons.

https://doi.org/10.5194/bg-2020-89
Preprint. Discussion started: 21 April 2020

Biogeosciences Discussions
Open Access
EGU

Table 2. Principal-components analysis (PCA) for the relationships between the gross primary productivity (GPP) and the environmental factors at the seasonal scale. Because there was no plant photosynthesis in winter, we did not perform the PCA for that season. PC, principal component; T_{air}, air temperature; R_n, net solar radiation; SHF, soil heat flux; SWC, soil water content; T_{soil}, soil temperature.

Component[a]	Spring			Summer			Autumn			
	PC1	PC2	PC3	PC1	PC2	PC3	PC1	PC2	PC3	PC4
T_{air}	0.849	0.410	0.108	0.431	0.849	-0.096	0.736	0.594	0.178	-0.004
Wind speed							0.023	-0.001	0.011	0.980
Rn	0.511	0.550	0.136	0.781	0.027	0.080	0.557	0.597	0.115	-0.299
SHF at 5 cm	0.138	0.967	-0.059	0.920	0.173	-0.134	0.928	0.057	-0.091	-0.007
SHF at 10 cm	0.191	0.951	0.032	0.932	0.185	-0.052	0.943	0.096	-0.063	0.071
SWC at 0-10 cm	0.184	-0.006	0.974	-0.073	-0.256	0.890	0.133	0.758	0.244	0.007
SWC at 10-50 cm	0.836	0.103	0.416	0.010	-0.017	0.933	0.000	0.848	-0.071	0.060
Precipitation							-0.055	0.146	0.962	0.008
T_{soil} at 0-50 cm	0.974	0.126	0.029	-0.003	0.950	-0.170	0.558	0.685	0.206	-0.131
Percent of variance	38.847	33.358	16.530	35.926	25.057	24.689	32.594	27.846	12.117	11.960
Cumulative	38.847	72.205	88.735	35.926	60.984	85.673	32.594	60.441	72.558	84.518

[a] Before the PCA, SWC was divided into two depth ranges (0 to 10, and 10 to 50) according to the results of a collinearity test for the four seasons. T_{soil} was divided into a single range (0 to 50 cm) according to the results of a collinearity test for the different seasons.

https://doi.org/10.5194/bg-2020-89
Preprint. Discussion started: 21 April 2020

Table 3. Principal-components analysis (PCA) for the relationships between the ecosystem respiration (R_{ec}) and the environmental factors at the seasonal scale. PC, principal component; T_{air}, air temperature; R_n, net solar radiation; SHF, soil heat flux; SWC, soil water content; T_{soil}, soil temperature.

Component[a]	Spring			Summer			Autumn			Winter		
	PC1	PC2	PC3	PC1	PC2	PC3	PC1	PC2	PC3	PC1	PC2	PC3
T_{air}	0.844	0.429	0.040	-0.064	0.912	0.141	0.726	0.603	0.179	0.333	0.891	0.071
Wind speed				0.010	0.030	0.995				0.057	0.230	0.730
R_n	0.615	0.334	-0.460				0.554	0.627	0.118	-0.106	0.320	-0.784
SHF at 5 cm	0.162	0.952	-0.197				0.928	0.066	-0.087			
SHF at 10 cm	0.234	0.929	-0.198				0.940	0.100	-0.061	-0.206	0.928	-0.090
SWC at 0-10 cm				0.811	-0.312	-0.091	0.123	0.754	0.248			
SWC at 10-50 cm				0.884	-0.106	-0.013	-0.012	0.838	-0.066			
SWC at 20-30 cm										0.868	0.053	-0.144
SWC at 20-50 cm	0.916	0.061	0.054									
SWC at 30-40 cm										0.949	-0.011	0.161
SWC at 40-50 cm										0.880	-0.110	0.144
Precipitation	0.116	-0.219	0.924	0.622	0.100	0.075	-0.057	0.139	0.964			
T_{soil} at 0-50 cm	0.946	0.124	0.050	-0.092	0.942	-0.091	0.549	0.702	0.207	0.735	0.390	0.244
Percent of variance	41.703	30.452	16.451	30.642	30.638	17.189	36.254	31.924	13.694	39.212	24.720	16.088
Cumulative	41.703	72.155	88.606	30.642	61.279	78.469	36.254	68.178	81.872	39.212	63.933	80.021

[a] Before the PCA, SWC was divided into six depth ranges (0 to 10, 10 to 50, 20 to 30, 20 to 50, 30 to 40, and 40 to 50 cm) according to the results of a collinearity test for the four seasons. T_{soil} was divided into a single range (0 to 50 cm) according to the results of a collinearity test for the different seasons.